Carbohydrate Polymers 115 (2015) 305–316

Contents lists available at ScienceDirect

Carbohydrate Polymers

journal homepage: www.elsevier.com/locate/carbpol

Rice starch granule amylolysis – Differentiating effects of particle size, morphology, thermal properties and crystalline polymorph

Sushil Dhital[a], Vito M. Butardo Jr.[b,1], Stephen A. Jobling[b], Michael J. Gidley[a,*]

[a] Centre for Nutrition and Food Sciences, ARC Centre of Excellence in Plant Cell Walls, Queensland Alliance for Agriculture and Food Innovation, The University of Queensland, St Lucia, QLD 4072, Australia
[b] Plant Industry and Food Futures Flagship, Commonwealth Scientific and Industrial Research Organisation (CSIRO), P.O. Box 1600, Canberra, ACT 2601, Australia

ARTICLE INFO

Article history:
Received 21 July 2014
Received in revised form 12 August 2014
Accepted 13 August 2014
Available online 2 September 2014

Keywords:
Amylopectin
Amylose
Amylose Extender
Digestibility
High amylose
Starch structure

ABSTRACT

The underlying mechanism of amylolysis of rice starch granules was investigated using isolated starch granules from wild-type, as well as *SBEIIb* mutant and down-regulated lines. Fused granule agglomerates isolated from mutant and transgenic lines were hydrolysed at similar rates by amylases, and had similar crystalline patterns and thermal properties as individual granules. Surface pores, a feature previously only reported for A-polymorphic starch granules, were also observed in B- and C-polymorphic rice starch granules. Although the microscopic patterns of hydrolysis among granules with different crystalline polymorphs were qualitatively similar, the extent and the rate of amylolysis were different, suggesting that B-type crystalline polymorphs are intrinsically more resistant to enzymatic hydrolysis than A-type in rice starch granules. It is proposed that the slightly longer branch lengths of amylopectin which leads to the formation of more stable B-type double helical structures compared to their A-type counterparts is the major parameter, with other factors such as granule size, surface pores and interior channels having secondary roles, in determining the rate of enzymatic hydrolysis of rice starch granules.

1. Introduction

The rate and extent of enzymatic hydrolysis of starch has attracted much attention not only due to its central role in converting starch to glucose as the major source of energy in human and animal diets, but also as an important biological (e.g. germination of grains and sprouting of tubers) and industrial process (e.g. syrups and bio-ethanol production). The action of amylolytic enzymes on starch granules may be affected by various factors including granule morphology (e.g. shape and size, presence of compound granules), surface features (e.g. surface damage, pores leading to interior channels, and other as yet incompletely characterised zones of enzyme susceptibility), presence of non-starch components (e.g. proteins, lipids and cell wall remnants), and molecular composition and conformation (e.g. size and amount of amylose and amylopectin, type and amount of crystallinity) as described elsewhere (Bird, Lopez-Rubio, Shrestha, & Gidley, 2009; Colonna, Leloup, & Buleon, 1992; Gallant, Bouchet, Buleon, & Perez, 1992). However, the relative importance of these factors has been difficult to determine as they are typically correlated with each other, and there is a lack of systems available for which individual factors vary whilst other factors are kept constant.

Starch has a broad array of granule sizes ranging from ca. 1 μm (e.g. rice, amaranth, and quinoa starch) to more than 100 μm (e.g. potato and canna starch). Smaller granules, either from different botanical origins (Fukai, Takaki, & Kobayashi, 1994; Ring, Gee, Whittam, Orford, & Johnson, 1988) or fractionated from the same origin (Dhital, Shrestha, & Gidley, 2010; Franco & Ciacco, 1992; Franco, Ciacco, & Tavares, 1998; Noda et al., 2005; Tang, Ando, Watanabe, Takeda, & Mitsunaga, 2001), are found to be more susceptible to amylolysis than their larger counterparts, consistent with the relatively higher surface area per unit mass available for enzyme adsorption (Warren, Royall, Gaisford, Butterworth, & Ellis, 2011). Cracks, holes or surface damage in granules can further increase the effective surface area enhancing the rate of enzymatic adsorption and binding to macromolecules. Cereal starches such as maize and sorghum are known to have naturally occurring surface pores and interior channels (Fannon, Hauber, & BeMiller,

* Corresponding author. Tel.: +61 7 33652145; fax: +61 7 33651177.
E-mail addresses: s.dhital@uq.edu.au (S. Dhital), v.butardo@irri.org (V.M. Butardo Jr.), steve.jobling@csiro.au (S.A. Jobling), m.gidley@uq.edu.au, mike.gidley@uq.edu.au (M.J. Gidley).
[1] Present address: International Rice Research Institute, Los Baños 4031, Philippines.

http://dx.doi.org/10.1016/j.carbpol.2014.08.091
0144-8617/

1992; Fannon, Shull, & BeMiller, 1993) that may facilitate the enzymes inside the granules affecting the hydrolysis rate and pattern compared to tuber and high amylose maize starches (HAMS), which apparently lack such structural features. Due to the easy access of enzymes towards the less organised granule interior, cereal starches are hydrolyzed at a faster rate from the inside to the outer periphery regions in an 'inside-out' pattern, whereas potato and HAMS granules are hydrolyzed more slowly by exo-corrosion, starting from the surface towards the inside of granules, an 'outside-in' pattern (Gallant, Bouchet, & Baldwin, 1997; Gallant et al., 1992; Zhang, Ao, & Hamaker, 2006). Indeed, the larger "A" granules from cereals such as wheat and barley have clear inbuilt zones of susceptibility to amylolysis around the equatorial groove which facilitates enzyme access for 'inside-out' digestion.

At shorter length scales, the distribution of semi-crystalline and crystalline layers based on double helices formed from amylopectin branches and molecular interaction within and between these layers may also affect the rate and extent of enzymatic hydrolysis. Double helices derived from shorter amylopectin branches (e.g. DP 10–12) form A-type crystallites as found in many cereal starches which may be more readily digestible than the B type crystallites containing longer double helices that are typical of tuber and high amylose cereal starches (Jane, Wong, & McPherson, 1997; Zhang, Venkatachalam, & Hamaker, 2006). However, the presence of surface pores and internal channels in many cereal starch granules, but not tuber and HAMS granules, may also be the rate-determining factor.

Thus, enzymatic hydrolysis of starch granules may be controlled by either the granular structure and/or the organisation of crystallites within the granules. These two factors however have not been investigated separately. Comparative study of potato and HAMS versus cereal starches such as maize or sorghum necessarily compares not only A-type vs. B-type polymorphs but also large differences in either amylose content (HAMS) and/or amylopectin branch lengths (potato) compared with most cereal starches. Indeed, differences in enzyme digestion between maize starches (waxy, normal and HAMS, with amylose contents from almost zero to more than 50%) (Evans & Thompson, 2004; Gerard, Colonna, Buleon, & Planchot, 2001; Morita, Ito, Brown, Ando, & Kiriyama, 2007), although representing the same botanical source, are difficult to assign a structural origin for as there are correlated sets of differences in terms of granular structure and molecular organisation. Furthermore, the study of enzymatic hydrolysis using crystalline substrates such as lintners (crystalline residues of starch after long mild acid hydrolysis) or amylose spherocrystals (e.g. crystallised de-branched amylopectin chains) may not be representative of the lamellar structure of native starch granules and results are often discordant. As an example, Planchot, Colonna, and Buleon (1997) reported A-type spherocrystals to be more readily hydrolyzed compared to B-type spherocrystals, whereas recently Cai and Shi (2013, 2014) showed the opposite effects for a different source of spherocrystals and crystalline aggregates. Thus, the underlying mechanism and factors contributing towards the enzymatic hydrolysis of starch granules are not fully understood.

In this paper, we report the effect of particle size and crystalline polymorph on the amylolysis of a series of related rice starches isolated from wild-type lines compared with mutant and transgenic lines where starch branching enzyme IIb (SBEIIb) is either absent or down-regulated. We previously described the structural, physico-chemical and functional impacts of down-regulating the levels of SBEIIb in rice using artificial microRNA (ami-RNA) and hairpin RNA (hp-RNA) RNA silencing techniques (Butardo et al., 2011). Rice altered by the ami-RNA technique (ami-BEIIb) produced a different starch phenotype to that modified using the hp-RNA technique (hp-BEIIb), with a slightly greater increase in the proportion of long amylopectin and intermediate chains. This resulted in a transition from the normal A-type starch crystalline pattern of the wild type Nipponbare to the C-type for hp-BEIIb and to the B-type for ami-BEIIb. This gives an opportunity to study the amylolysis of starches from cultivars of a single species (*Oryza sativa Japonica* ssp. Nipponbare cultivar) with similar amylose content but with different crystalline polymorphs, to elucidate the underlying mechanism and factors contributing towards the enzymatic hydrolysis of granular rice starches. We also compare the rate of enzymatic hydrolysis for *Indica* rice ssp. wild-type (IR36) and its corresponding *amylose extender* (IR36ae) mutant which was previously shown to have elevations in true amylose, as well as having significantly elevated proportions of long chain amylopectin and intermediate chains (Butardo et al., 2012)

2. Materials and methods

2.1. Materials

Two wild type rice lines were used as reference controls in this study, one in a *Japonica* background (Nipponbare, NIP) and one in an *Indica* background (IR36). They were compared with hp-BEIIb and ami-BEIIb transgenic lines with down-regulated *SBEIIb* generated by *Agrobacterium* transformation of the *Japonica* parent line NIP using hairpin RNA (hp-RNA) and artificial microRNA (ami-RNA) RNA silencing, respectively. We also used IR36ae, an *SBEIIb* mutant of the *Indica* parent line IR36 to serve as a reference control for high amylose rice *amylose extender* mutation.

All the transgenic Nipponbare rice lines used in this study were previously developed in CSIRO Plant Industry (CPI), Canberra, Australia (Butardo et al., 2011). Nipponbare, IR36 and IR36ae were routinely grown in CPI, from the seed stocks originally obtained from Yanco Agricultural Institute, Yanco, NSW, Australia. All the rice lines were simultaneously grown inside a biosafety glass house for this experiment as previously described (Butardo et al., 2011). Mature panicles were harvested, dried, threshed and dehulled, after which the seeds were polished and milled to generate the rice flours used in this study.

2.2. Methods

2.2.1. Isolation and fractionation by sedimentation

Starch was isolated from various rice lines following alkali extraction of the protein. 15 g of milled rice was steeped in 6 volumes of 0.165% (w/v) sodium hydroxide solution (Cardoso, Putaux, Samios, & da Silveira, 2007) at room temperature (ca. 22 °C) for 24 h to soften the endosperms. The steep liquor was drained off and the endosperms were ground lightly into successively smaller fractions using a mortar and pestle. The slurry was then diluted to the original volume with 0.165% (w/v) sodium hydroxide, stirred for 10 min and allowed to settle overnight. The cloudy supernatant (70 mL) was drained off, and the sediment was again diluted to the original volume with 0.165% sodium hydroxide solution. The mixture was then shaken for 10 min and centrifuged at 1250 rpm for 5 min. The process was repeated until the supernatant became clear and gave a negative reaction to the Biuret test for protein. The slurry of starch was suspended in distilled water, passed through a 250 μm sieve and centrifuged at 1200 rpm for 5 min. The washing process was repeated until no pink colour was observed in the presence of phenolphthalein, and finally starches were washed with ethanol and dried overnight at 40 °C under vacuum.

The isolated granules were separated into very small (VS, <4 μm diameter (Ø)), small (S, 4–6 μm Ø), medium (M, 6–8 μm Ø) and large (L, >8 μm Ø) fractions by a repeated sedimentation process in water containing 0.02% sodium azide (Dhital et al., 2010b). The relative yield and median diameter of separated fractions measured

Table 1
Relative yield and median size of starch fractions.

Varieties	Relative yield (%)				Median particle size (μm)				
	VS	S	M	L	Native	VS	S	M	L
Japonica lines									
ami-BEIIb	35.84	19.88	16.12	18.23	4.78	3.54	4.63	5.70	11.18
hp-BEIIb	23.52	31.90	21.92	9.91	4.58	3.63	4.92	5.33	6.60
NIP	21.06	46.80	28.33	2.12	4.90	4.11	4.91	5.83	7.32
Indica lines									
IR36	10.23	45.79	35.61	6.11	6.20	4.92	5.52	6.25	6.75
IR36ae	11.33	20.57	18.97	49.14	9.32	3.57	4.86	6.63	11.96

VS = very small; S = small; M = medium; L = large.

by light scattering (Malvern Mastersizer Hydro 2000MU) are presented in Table 1. At least 10 sedimentation repeats were required for efficient separation of each fraction, and the sedimentation time per run was 6.4, 2.8, and 1.6 h for VS, S and M fractions respectively.

2.2.2. Microscopic observation, diffraction pattern and thermal properties

Electron micrographs of isolated starch and enzyme digested residue were obtained as described previously (Dhital, Shrestha, & Gidley, 2010). The internal structure of granules and agglomerates was observed using a confocal microscope after labelling with APTS as described previously (Dhital, Shelat, Shrestha, & Gidley, 2013). Multiple micrographs of each sample were examined at multiple magnifications, and typical representative images selected.

The crystalline pattern and thermal properties of starch fractions were determined by using a X-ray diffractometer and a differential scanning calorimeter as previously described (Dhital, Shrestha, Hasjim, & Gidley, 2011; Shrestha et al., 2012).

2.2.3. Enzymatic hydrolysis

Starch fractions (~45 mg each, in duplicate) were hydrolyzed using porcine pancreatin (Sigma P1750, 20 mg per gram of starch) and fungal amyloglucosidase (Sigma A-7420, 280 units per gram of starch) in 0.2 M sodium acetate buffer (pH 6, 70 mL per gram of starch) for 30, 60, 180, 300, and 360 min in 50 mL falcon tubes partially immersed in a water bath at 37 °C (above a hotplate magnetic stirrer) with continuous stirring at 200 rpm with a 10 mm × 3 mm micro PTFE coated magnetic stirrer. The enzymatic activity was stopped after the completion of each digestion time by adding 4 volumes of absolute ethanol. The glucose concentration in the supernatant was determined by using a glucose oxidase colorimetric analysis kit (TR-1511-200 Thermo Electron Noble Park, Victoria, Australia) and the factor 0.9 was used to convert anhydrous glucose released to the percentage starch hydrolysis. The residue after repeated washing (×3) was dried under vacuum at 40 °C and observed using scanning electron microscopy as described previously (Dhital et al., 2010a).

2.2.4. Statistical analysis

The Minitab® ver16 software (Minitab Inc., State College, PA 16801-3008, USA) was used for analysis of variance (ANOVA) and tests of significance at 95% confidence level from at least two technical replicates.

3. Results

3.1. Granule size and size distribution

The yield and median size of starch granule fractions are shown in Table 1 and the size distribution pattern is shown in Fig. 1. Scanning electron micrographs of unfractionated granules are shown in Fig. 2. Wild-type starches (NIP and IR36) are all polyhedral and predominantly similar-sized individual granules. In contrast, mutant and transgenic lines are less regularly shaped and include fused agglomerated granules, particularly for IR36ae and ami-BEIIb, characteristic of starch with elevated apparent amylose. This form of isolated starch granules are referred to as semi-compound granules by some authors (Wei et al., 2010) to distinguish them from apparent compound granules formed by the close packing of intact starch granules within the amyloplast. While compound granules from wild type rice starches disassociate into single (simple) granules during starch isolation, fused granule agglomerates (semi-compound granules) from high amylose rice lines stay intact after isolation (Fig. 2).

Size separation through sedimentation was successful for IR36ae and ami-BEIIb, but less so for other lines (Fig. 1). This is consistent with separation of fused granule agglomerates from individual granules, but limited fractionation of individual granules, possibly due to their relatively small size and the correspondingly long sedimentation times required resulting in inefficient fractionation. Among transgenic lines, ami-BEIIb contains more fused granule agglomerates than hp-BEIIb whereas the mutant IR36ae had the highest apparent proportion of the starches studied (Fig. 2). This result is consistent with the previous observation that amiRNA silencing produced starch granules more closely resembling the full *SBEIIb* mutant (IR36ae) than the hp-RNA method (Butardo et al., 2011).

Compared at the level of individual isolated starch granules, wild-types have polyhedral structures together with smooth granule surfaces and edges compared to mutant and transgenic lines which are more rounded and have mostly rough surfaces and cracked/damaged edges. The fused granule agglomerates detected in mutant and transgenic lines have undulating structures with cracks and fissures on the surface, and are internally packed with approximately hexagonal sub-granules surrounded by a continuous band (Fig. 2F). Surface pores are observed in starch granules of all lines, with comparatively fewer but larger sized pores present in wild-types compared to mutant and transgenic lines (Fig. 2 insets).

3.2. Crystalline pattern

The X-ray diffraction patterns are very similar for sedimentation fractions from individual lines but different between lines (Fig. 3). Sedimentation fractions of wild-types (NIP and IR36) have the typical A-type diffraction pattern with signature peaks corresponding to Bragg angles (2θ): 15°, 17°, 18° and 23° whereas the B-type crystalline pattern was prominent in IR36ae and ami-BEIIb with characteristic peaks at ~5.5° and 17° 2θ. In contrast, the size fractions of hp-BEIIb have a typical C-type diffraction pattern which is intermediate between the A- and B-type patterns, including diffraction peaks at both 23° and 5.5° 2θ. A slightly elevated 20° 2θ peak is observed in IR36ae and ami-BEIIb lines representing the V-type diffraction pattern. These findings are consistent with previous

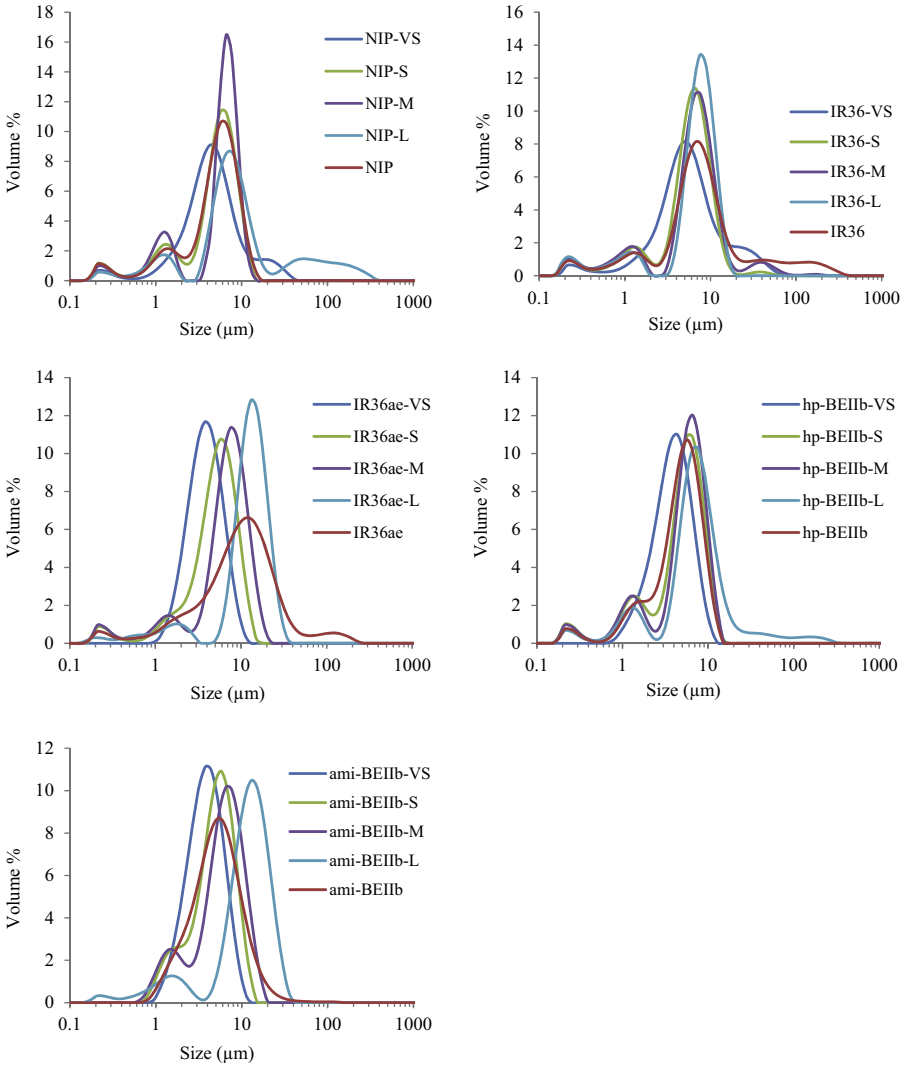

Fig. 1. Granule size distribution of starches in water measured by laser light scattering.

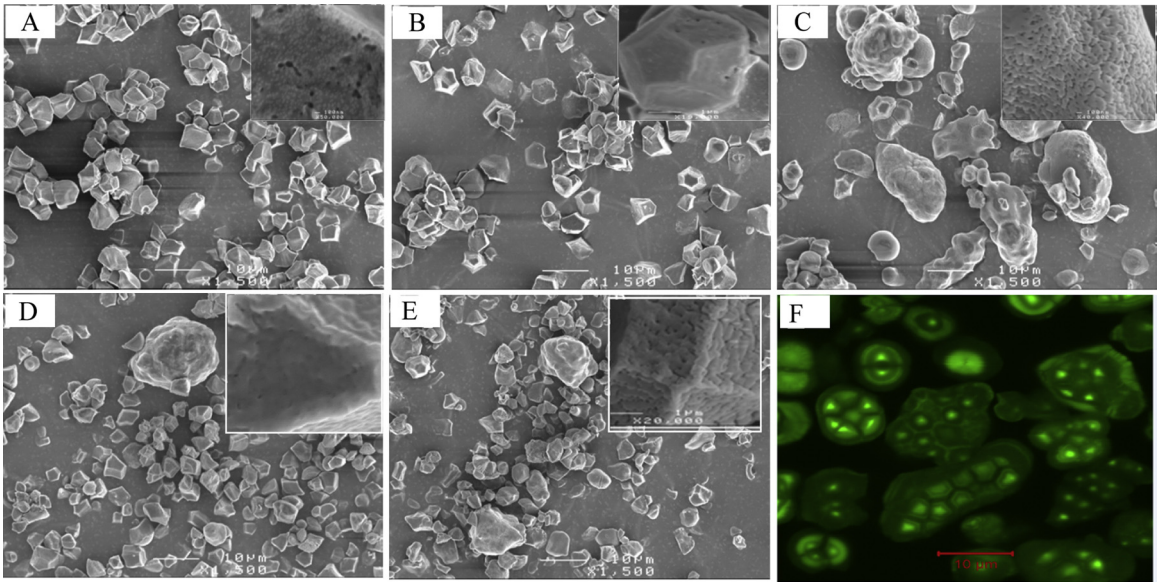

Fig. 2. Representative electron micrographs of unfractionated starches at 1500× magnification. A: NIP; B: IR36; C: IR36ae; D: hp-BEIIb; E: ami-BEIIb; F: confocal micrograph of IR36ae showing internal structures in semi-compound granule. Surface pores in granules are shown in insets A–E.

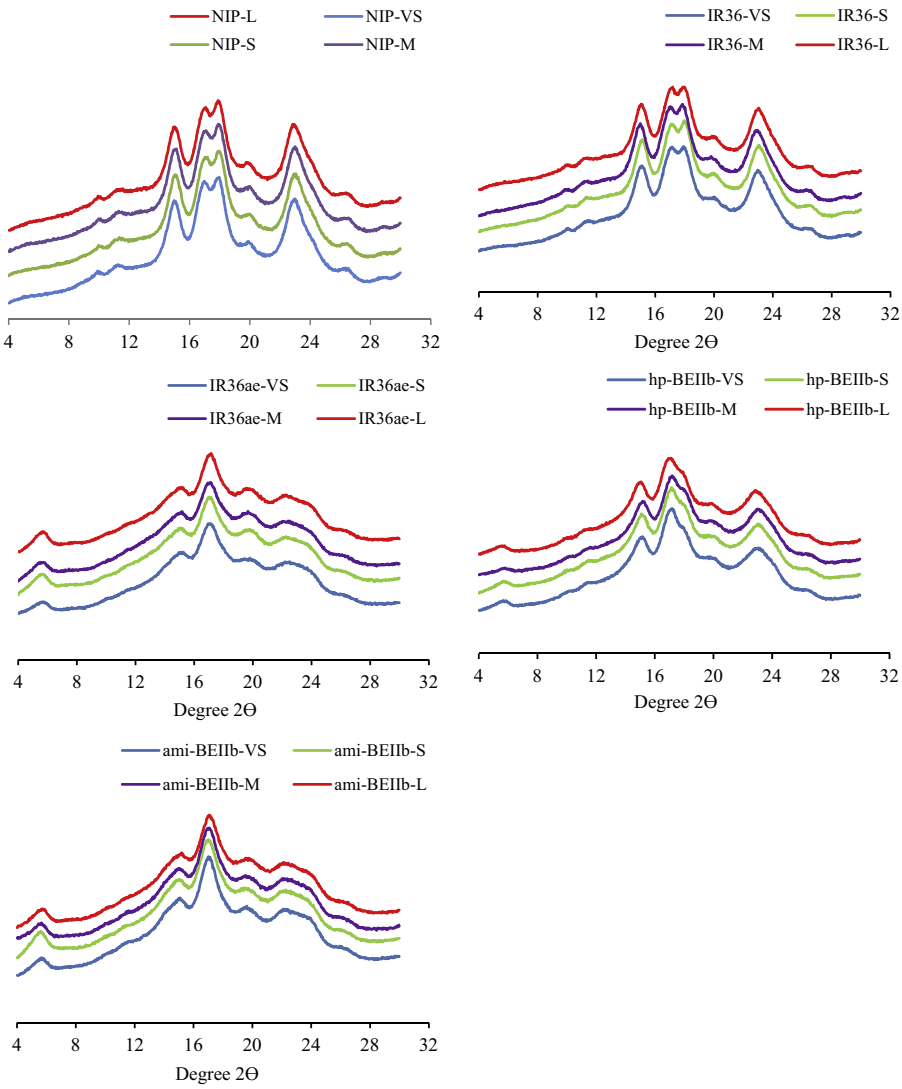

Fig. 3. X-ray diffraction pattern of size fractionated starches. Data are off set for clarity.

results for unfractionated rice flour samples for each line (Butardo et al., 2011).

3.3. Thermal properties

Differences in thermal properties among starch varieties and sedimentation fractions (L and VS) are observed (Table 2). The thermal parameters were almost similar among SBEIIb transgenic Japonica lines (ami-BEIIb and hp-BEIIb) but were significantly higher in temperature, enthalpy (ΔH), and temperature spread (ΔT) compared to the parent line (NIP), suggesting that down regulation of *SBEIIb* leads to greater double helical content (enthalpy) and length (melting temperature). For *Indica* lines, the gelatinisation temperature range was almost 1.5 times greater for IR36ae compared to wild type IR36, mostly due to lower onset temperatures (T_o) as well as a lower ΔH for IR36ae compared to IR36, particularly for the large granule fractions. Small but significant differences were observed in thermal properties between the *Japonica* (NIP) and *Indica* (IR36) wild types. The melting of helices started and concluded at significantly lower temperatures in NIP than IR36, whereas the ΔT was higher for NIP, although ΔH were similar. This observation is consistent with differences in Starch Synthase IIa activity and the resulting amylopectin fine structure between NIP ('inactive' japonica-type *SSIIa* producing S-type amylopectin) and IR36 ('active' Indica-type *SSIIa* producing L-type amylopectin) (Nakamura et al., 2005).

Among sedimentation fractions, T_o of VS fractions compared to the L fractions was slightly but significantly lower for wild types but the reverse was true for transgenic lines. However such a demarcation was not observed for peak (T_p) and conclusion temperatures (T_c), and all differences are relatively minor in magnitude. The ΔH and ΔT are similar for L and VS sedimentation fractions with some exceptions such as the L fraction of IR36 having significantly higher ΔH but lower ΔT compared to VS fractions.

3.4. Amylolysis kinetics

The hydrolysis kinetics of starches and their sedimentation fractions are shown in Fig. 4. All the varieties have monophasic digestograms, characteristic of gradual depletion of substrate (represented as % starch hydrolysis) with increase in time. Such a decay phenomenon can be well fitted by first order kinetics. The digestion rate coefficients, an absolute value of slope of first order fits of decay plots, are shown in Table 3, determined using a previously described method (Al-Rabadi, Gilbert, & Gidley, 2009; Dhital et al., 2010b; Zhang, Dhital, & Gidley, 2013).

Among the starches, NIP is more rapidly digested followed by IR36, IR36ae, hp-BEIIb and ami-BEIIb. For example, after 6 h (Fig. 4),

Table 2
Thermal properties of large (L) and very small (VS) fractions of starches.[1]

Parameters		T_o	T_p	T_c	ΔH	ΔT
Japonica lines						
ami-BEIIb	L	67.89 (0.01)^{d}	76.74 (0.11)^{a}	84.12 (0.07)^{b}	13.65 (0.49)^{ab}	16.23 (0.06)^{a}
	VS	70.23 (0.17)^{b}	77.17 (0.13)^{a}	85.16 (0.25)^{a}	15.24 (0.18)^{a}	14.93 (0.08)^{b}
hp-BEIIb	L	67.69 (0.06)^{d}	75.72 (0.13)^{b}	82.50 (0.21)^{c}	14.76 (0.41)^{a}	14.81 (0.27)^{b}
	VS	69.25 (0.01)^{c}	76.85 (0.06)^{a}	83.54 (0.06)^{b}	15.58 90.63)^{a}	14.30 (0.05)^{bc}
NIP	L	63.57 (0.01)^{f}	69.01 (0.01)^{e}	74.68 (0.13)^{g}	10.53(0.59)^{cde}	11.11 (0.14)^{d}
	VS	61.56 (0.02)^{g}	68.09 (0.11)^{f}	76.20 (0.40)^{f}	11.56 (0.69)^{bcd}	13.15 (0.42)^{b}
Indica lines						
IR36ae	L	65.75 (0.13)^{e}	73.55 (0.11)^{cd}	80.26 (0.35)^{d}	6.11 (0.84)^{f}	14.51 (0.22)^{bc}
	VS	66.17 (0.24)^{e}	72.93 (0.11)^{d}	79.72 (0.01)^{de}	8.24 (0.16)^{ef}	13.55 (0.25)^{c}
IR36	L	71.93 (0.49)^{a}	75.59 (0.25)^{b}	79.48 (0.05)^{de}	13.09 (1.00)^{abc}	7.55 (0.54)^{f}
	VS	69.54 (0.14)^{bc}	73.89 (0.32)^{c}	78.87(0.42)^{e}	9.12 (1.36)^{de}	9.33 (0.28)^{e}

[1] Values are expressed as mean (standard deviation) of at least duplicate analyses. Means that do not share a letter in each column are significantly different at $p = 0.05$. T_o, T_p and T_c correspond to onset, peak and conclusion gelatinisation temperature (°C) whereas ΔH and ΔT represent melting enthalpy (J/g of starch) and gelatinisation temperature range (°C) respectively.

almost all NIP is hydrolysed whereas only 50% of ami-BEIIb is hydrolysed. Comparing the amylolysis extent between parent and mutant or transgenic lines, the difference between IR36 and IR36ae is comparatively less than that of NIP compared with hp-BEIIb and ami-BEIIb, consistent with a greater starch structural difference between NIP and the high apparent amylose starches in NIP backgrounds than between IR36 and IR36ae (Butardo et al., 2012, 2011). Furthermore, among transgenic lines, starch obtained from down

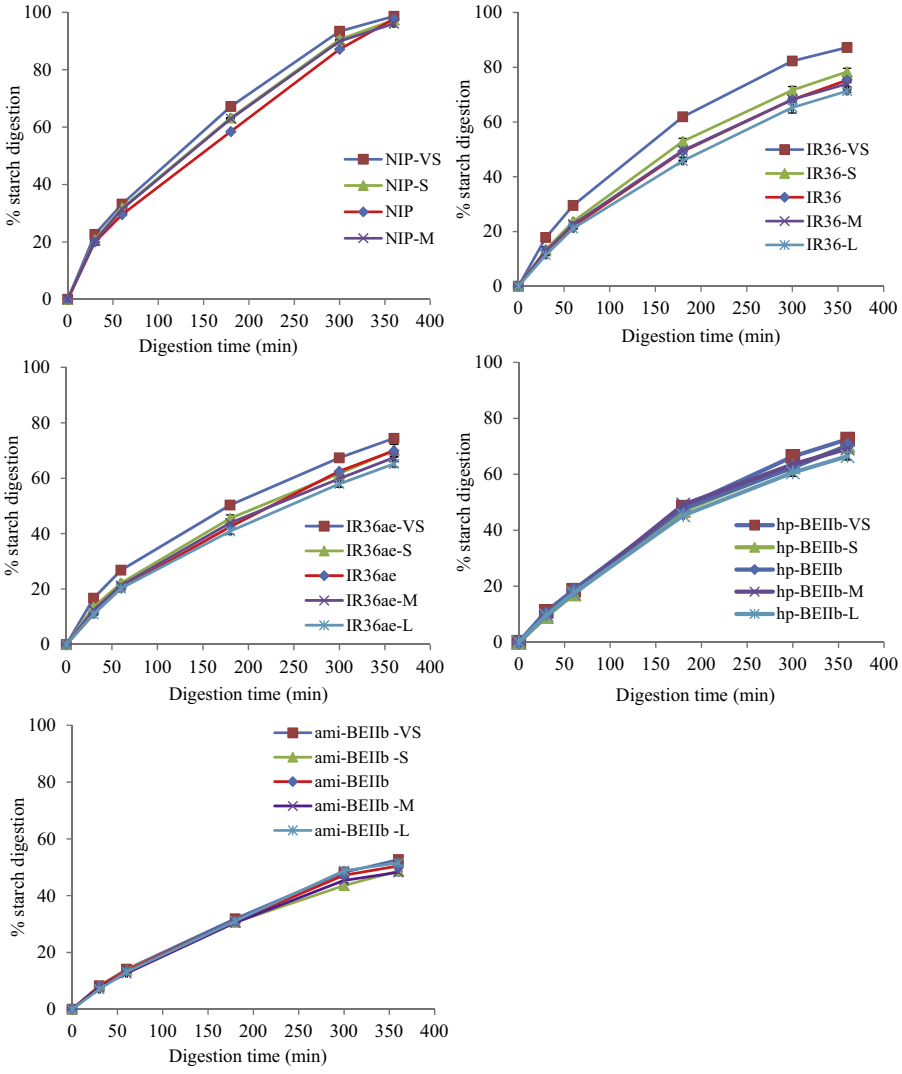

Fig. 4. In vitro digestion kinetics of starches with porcine pancreatin. The L fraction of NIP was excluded due to lack of sufficient amount of sample.

Table 3
Digestion rate coefficients (min^{-1}) from fitting first order kinetics to digestograms.[1,2]

Size	NIP	IR36	IR36ae	hp-BEIIb	ami-BEIIb
L	–	3.4E−03 (4.3E−05)^{c1}	2.8E−03 (9.4E−05)^{c2}	3.0E−03 (1.0E−04)^{c2}	2.0E−03 (6.6E−05)^{a3}
M	8.5E−03 (1.6E−05)^{a1}	3.7E−03 (1.0E−04)^{bc2}	3.0E−03 (1.2E−04)^{bc3}	3.3E−03 (7.3E−05)^{bc3}	1.8E−03 (3.2E−05)^{b4}
S	9.3E−03 (1.3E−05)^{a1}	4.1E−03 (1.6E−04)^{b2}	3.2E−03 (1.1E−04)^{b3}	3.3E−03 (1.6E−04)^{ab3}	1.8E−03 (7.7E−05)^{b4}
VS	1.1E−02 (1.8E−05)^{a1}	5.6E−03 (1.2E−04)^{a2}	3.6E−03 (2.7E−04)^{a3}	3.6E−03 (4.6E−07)^{a3}	2.0E−03 (3.0E−05)^{a4}
Native	9.2E−03 (1.6E−05)	3.8E−03 (6.9E−05)	3.2E−03 (1.1E−04)	3.3E−03 (1.8E−05)	1.9E−03 (3.0E−05)

[1] Values are expressed as mean (standard deviation) of at least duplicate analyses. Means that do not share a letter in each column and number in each row are significantly different at $p = 0.05$.
[2] Significance difference are compared among sediment fractions only.

regulating *SBEIIb* by the hairpin RNA gene silencing technique (hp-BEIIb) is less resistant to amylolysis than that of artificial microRNA silencing technique (ami-BEIIb). This observation is consistent with our previous finding using a different amylase assay (hydrolysis index) which assessed *in vitro* digestibility of freshly cooked whole grains (Butardo et al., 2011).

Sedimentation fraction dependence of enzymatic hydrolysis is observed for IR36, IR36ae and hp-BEIIb, whereas differences are comparatively small in the case of NIP and ami-BEIIb (Fig. 4), despite the fact that the median diameter of the largest fraction of ami-BEIIb is almost double that of the smallest fraction. Comparing parent lines with related mutants, a significant difference in digestion rate coefficient was observed between NIP, hp-BEIIb and ami-BEIIb for all size fractions in the order of NIP > hp-BEIIb > ami-BEIIb and significant difference was also observed between IR36 and IR36ae. In our previous study, the digestion kinetics based on hydrolysis index measurement of freshly cooked polished grains of NIP was fastest followed by hp-BEIIb lines, with ami-BEIIb lines being the least digestible. The same is also true for the *Indica* lines where IR36 is more digestible than IR36ae (Butardo et al., 2011).

3.5. Amylolysis pattern

The digestion patterns of starches, regardless of granule size and polymorphic types, are all similar (Figs. 5–9). In the majority of granules, digestion appeared to occur through pores apparent at the surface of granules, with the potential for subsequent internal digestion where surface pores are connected to interior channels. However, the degree of hydrolysis as observed from the number and size of enlarged pores was not uniform among granules. For example, after 30 min hydrolysis of VS and M fractions of NIP (Fig. 5A1 and B1), granule pores are not evenly distributed, some are highly pitted whereas others are comparatively less pitted. However, after 1 h of hydrolysis (Fig. 5A2 and B2), the majority of granules have bigger holes and/or fractured surfaces, exposing the interior of granules. Similarly, highly pitted and fragmented granules are observed after 30 min and 3 h hydrolysis of VS and L fractions of hp-BEIIb (Fig. 8). The digestion of larger fused granule agglomerates, however, appears to be different from that of individual granules. For example in Figs. 7 and 9(B), after the first 30 min of hydrolysis, cracks in the surface due to enzymatic action are clearly visible. Some granules even opened up (i.e. disintegrated) (Fig. 9B1) during the hydrolysis process. However, the final hydrolysis pattern is similar to that of individual granules, involving enlarging of holes in the surface towards the granule interior leading to granule fragmentation.

4. Discussion

Differentiating the effects of particle size, morphology, thermal stability and crystalline polymorph on the rate of amylolysis of rice starch granules has been approached by studying isolated and sedimentation-fractionated granules from wild-type and related mutant and transgenic lines with defined differences in crystalline type and molecular structure as exemplars. Crystalline type, as influenced by amylopectin molecular structure, rather than granular structure features such as surface pores and interior channels, or fused agglomerates vs. simple granules was found to be consistently associated with differences in the rate of amylolysis of the granular rice starches studied. Furthermore, it has also been shown for the first time that B-type crystalline granules can have surface pores through which amylase [with hydrodynamic radius of ca 3–4 nm (Payan et al., 1980)] can access the granule interior, unlike other B-type granules such as HAMS and potato starch.

4.1. Granule size and shape

The biosynthesis of starch occurs in amyloplasts. Rice grain amyloplasts contain several starch granules (granula) tightly packed as apparently compound granules. Such granules are often rounded at first, but become angular as they pack together within the amyloplast. In our previous study, intact compound wild type starch granules appear angular and tightly packed while that of SBEIIb down-regulated lines appear rounded and loose with lots of air spaces in between (Butardo et al., 2011). These so-called compound granules are typically broken down during the starch extraction process releasing the individual polyhedral granules (Shapter, Henry, & Lee, 2008; Wei et al., 2010). The polyhedral granules of wild varieties (e.g. Fig. 2A and B) are thus derived from disintegrated compound granules. However, the mutant and transgenic lines have varying amount of large non-angular fused granule agglomerates (also referred to as semi-compound granules by some authors) in the decreasing order of IR36ae, followed by ami-BEIIb and hp-BEIIb. These agglomerates are also identified as compound granules in the grain, but the granules do not separate during starch extraction because they are fused together by a surrounding layer of apparently amorphous starch (Gott, Barton, Samuel, & Torrence, 2006) (Fig. 2F). The physiology of starch development and the formation of fused agglomerates and compound granules has been well described elsewhere (Shannon & Garwood, 1984). More recently, Wei et al. (2010) and Zhu, Liu, Wilson, Gu, and Shi (2011) also reported the presence of fused granule agglomerates (semi-compound granules) in transgenic high amylose rice with down-regulated SBEIIb and SBEI. Compared to NIP and IR36, the individual granules in fused agglomerates have damaged surfaces possibly as the result of fracturing during the extraction process. Though wild types were mostly individual granules, the isolated granule agglomerates from mutant and transgenic lines provide the opportunity for a comparative study of properties and enzyme susceptibility between individual granules and fused agglomerates.

4.2. Surface features

The surfaces of individual granules in all lines are found to have varying numbers of pores. These pores, some of which are linked to channels connecting outer surface to granule interiors, have previously been thought to be unique features of starches with A-type crystallinity as reported by Fannon et al. (1992), and are not

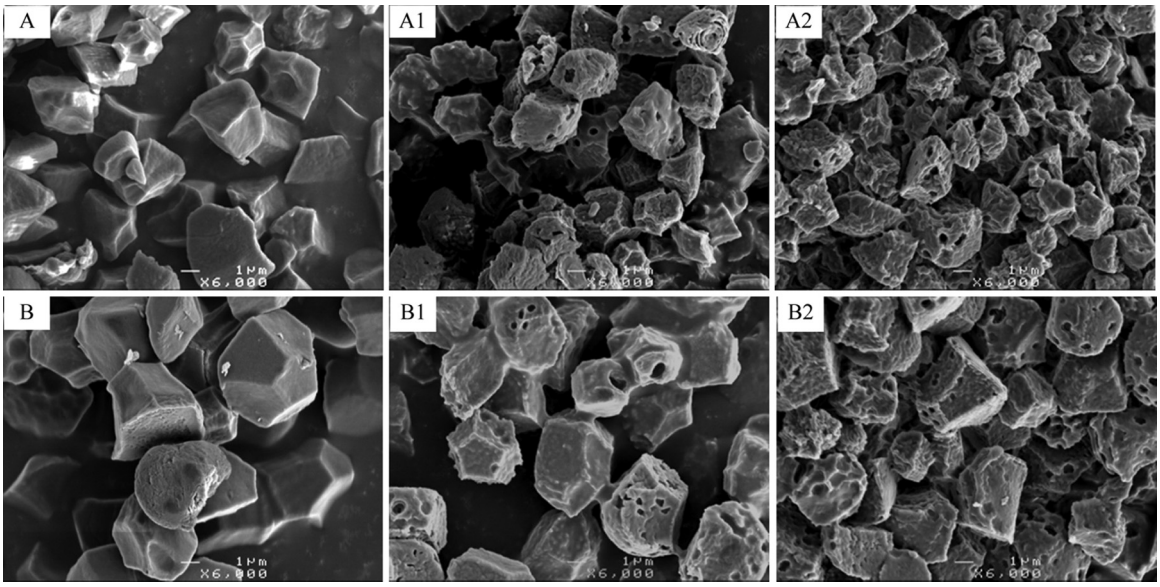

Fig. 5. Electron micrographs before and after in vitro digestion of NIP fractions. A and B: VS and M fraction (control), A1 and A2, B1 and B2: VS and M fractions after 30 min and 1 h in vitro digestion respectively.

observed in B-type starches such as potato and high amylose maize starches (Dhital et al., 2010a; Shrestha et al., 2012). We demonstrate for the first time the presence of pores in the surface of B-type (rice) starches (Fig. 2C–E insets). Channels of A-polymorphic starches are reported to contain proteins similar to those found in the amyloplast, suggesting that channels are natural features formed during the granules developing around radially oriented microtubules in the amyloplast (Benmoussa et al., 2010). However, this mechanism does not explain why surface pores and interior channels are not found in higher amylose cereal starches. As the study of pores and channels have previously involved only A-polymorphic starches, the current finding of pores in B- and C-polymorphic rice starches suggests that the crystalline polymorph is not the dominant factor determining the formation of pores and channels, at least in rice granules.

4.3. In vitro hydrolysis

The amylase hydrolysis patterns of all the rice lines, irrespective of crystalline type are similar, with formation and enlargement of surface pores and interior channels facilitating hydrolysis from the hilum region towards the outside of granules. The surface pores and possibly interior channels in all rice starches would allow easier access of amylase to the less organised granule interior (Huber & BeMiller, 2000), similar to what is found for maize and sorghum starches which are digested by an 'inside out' pattern. However, for starches without pores and channels, e.g. potato, the enzymes initiate digestion from the surface through 'exo pitting' (Gallant et al., 1992) as their surface is apparently impermeable to amylases The inside-out digestion pattern observed for B- and C-type starches in this study suggests that the surface features primarily determine

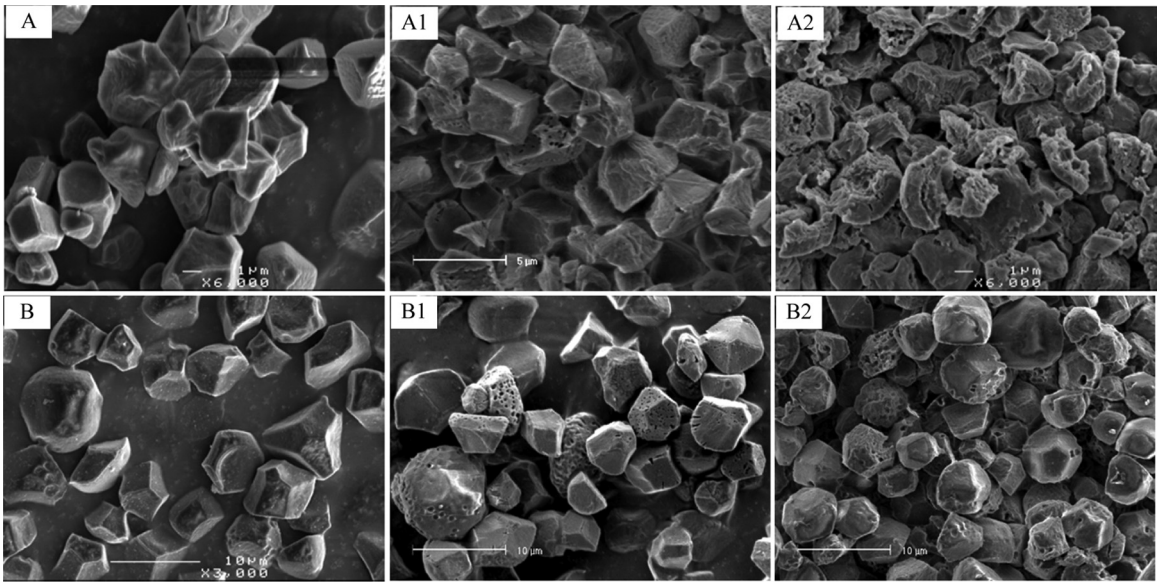

Fig. 6. Electron micrographs before and after in vitro digestion of IR36 fractions. A and B: VS and L fractions (control), A1 and A2, B1 and B2: VS and L fractions after 30 min and 3 h in vitro digestion respectively.

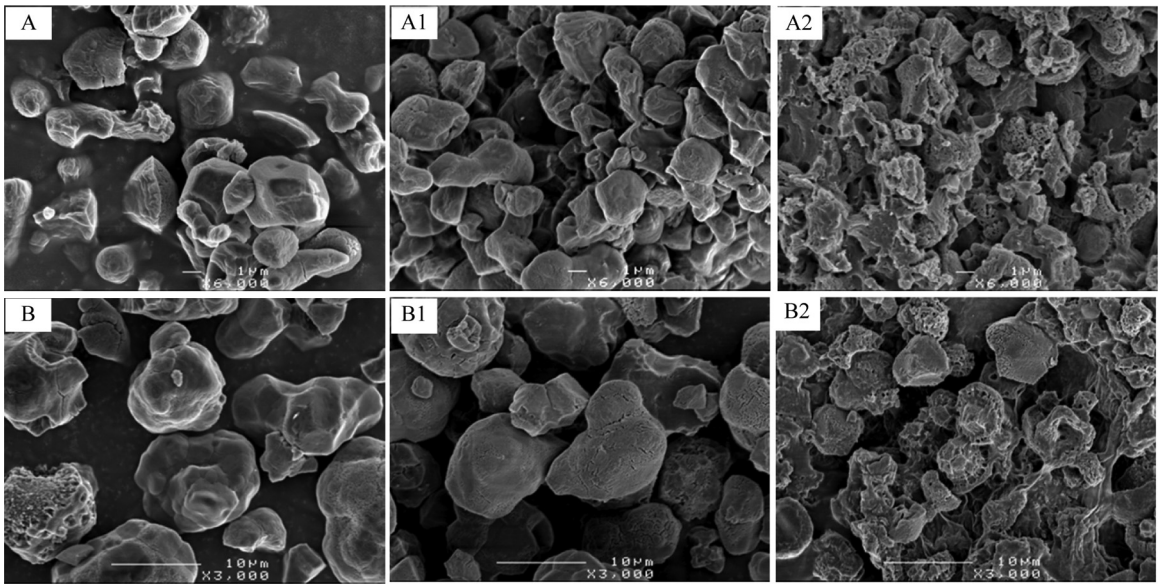

Fig. 7. Electron micrographs before and after in vitro digestion of IR36ae fractions. A and B: VS and L fractions (control), A1 and A2, B1 and B2: VS and L fractions after 30 min and 3 h in vitro digestion respectively.

the pattern of amylase hydrolysis of rice starch granules, although the SEM evidence (Figs. 5–9) is not as strong as that for maize starches due to the smaller size of rice granules. However, in spite of similarities in the pattern of hydrolysis, the extent of hydrolysis of rice starches is markedly different. As shown in Fig. 4 (digestion kinetics curves) and Table 3 (digestion rate coefficients), ami-BEIIb, a B-polymorph starch, has significantly lower amylase hydrolysis extent and rate compared to the parent A-polymorph NIP, although both lines have pores in their granule surfaces. Thus the presence of pores which appear to control the qualitative pattern of digestion can be associated with marked variations in the digestion extent and rate coefficients. Although crystalline types correlate with relative amylolysis rates between lines, they do not always reflect the same differences in amylolysis difference between lines. For example, the difference in amylolysis extent or digestion rate coefficient between parent IR36 (A-polymorph) and mutant IR36ae (B-polymorph) is comparatively less than that between NIP parent (A-polymorph) and transgenic ami-BEIIb (B-polymorph).

Nipponbare is in a *Japonica* background with an inactive form of SSIIa and GBSSI while IR36 is in an *Indica* background with an active form of both enzymes similar to the cultivar Kasalath used by Umemoto et al. (2004). *Japonica* lines, being low in amylose, are typically easier to digest than the usually higher amylose content *Indica* lines (Hu, Zhao, Duan, Linlin, & Wu, 2004). Despite these genotypic and starch functional differences, the starch granules of ami-BEIIb are still the least susceptible to amylolysis even though it has lower true amylose chains (Butardo et al., 2011) and *Japonica*-type SSIIa (Nakamura et al., 2005). In the case of ami-BEIIb (and hp-BEIIb), the proportion of true amylose chains is similar to the wild type NIP, whereas the proportion of long chain amylopectin

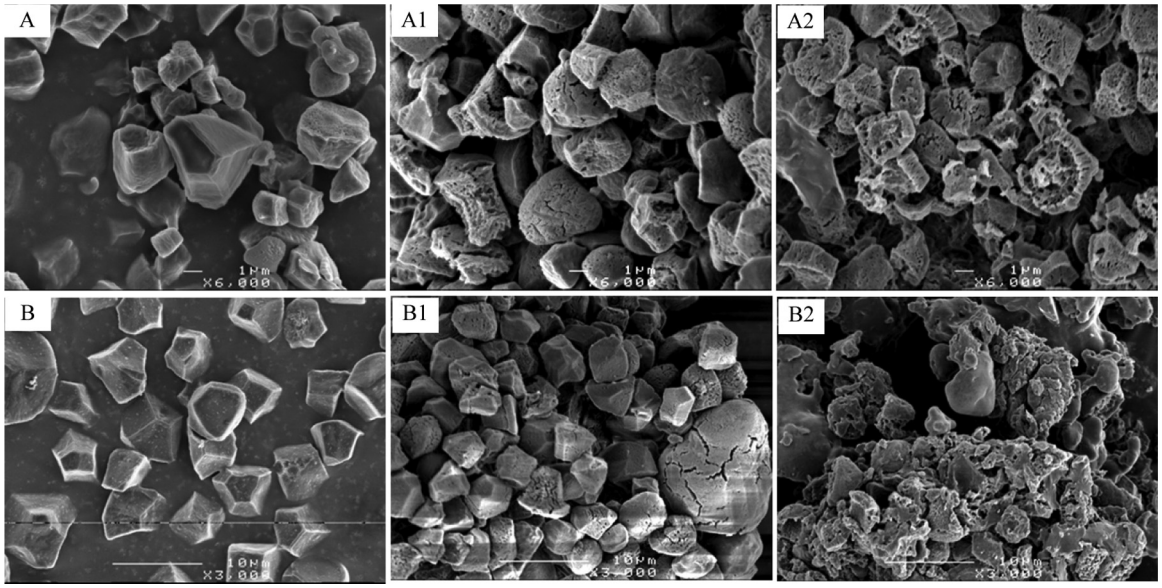

Fig. 8. Electron micrographs before and after in vitro digestion of hp-BEIIb fractions. A and B: VS and L fractions (control), A1 and A2, B1 and B2: VS and L fractions after 30 min and 3 h in vitro digestion respectively.

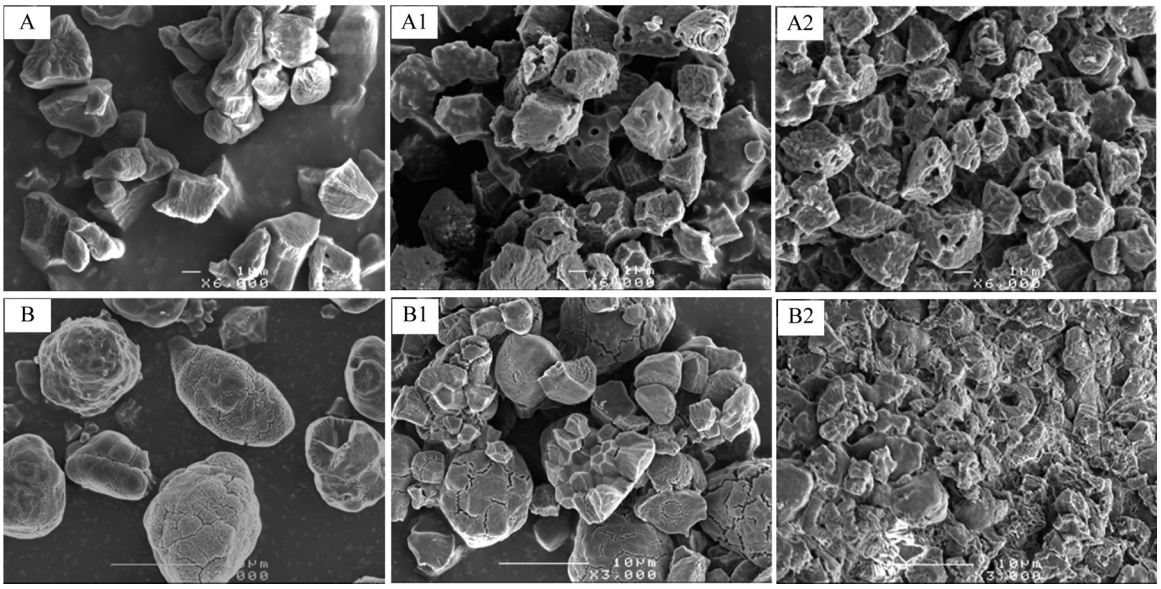

Fig. 9. Electron micrographs before and after in vitro digestion of ami-BEIIb fractions. A and B: VS and L fractions (control), A1 and A2, B1 and B2: VS and L fractions after 30 min and 3 h in vitro digestion respectively.

is elevated (Butardo et al., 2011). This indicates the importance of long chain amylopectin in determining resistance to amylolysis of rice starch granules.

To integrate these findings, we propose that the chain length distribution of amylopectin and amylose is the underlying feature that results in the relative effectiveness of amylase action towards rice starch granules. In previous publications, we reported the molecular size of wild type, mutant and transgenic starches (Butardo et al., 2012, 2011). Chain length distributions (CLDs) of debranched starches revealed a decrease in the proportion of amylopectin short chains (DP 6–12) with a concomitant increase in the longer chains (DP >14) in mutant and transgenic lines compared to wild types. Furthermore, the transgenic and mutant starches have comparatively long chain amylopectin which are capable of binding iodine thereby leading to up to twofold increase in the apparent amylose content of the transgenic lines compared to their wild type. In contrast, the true amylose chains, monitored by measuring iodine complex absorbance at 720 nm and by SEC, were similar for all rice varieties with the Nipponbare genetic background (Butardo et al., 2011). The longer amylopectin chains can extend through multiple clusters forming longer and more stable double helices that may be comparatively harder for amylase to access and/or hydrolyse compared to less stable shorter amylopectin chains. Thus, the amylase resistance of ami-BEIIb compared with the parent NIP may at least in part be due to amylopectin chain lengths either directly through greater double helical stability, or indirectly through effects on crystalline polymorph, although a difference in the nature and number of surface pores and interior channels cannot be excluded based on the current data.

4.4. Effect of granule size on amylase hydrolysis

The effects of granule size on amylase action (Dhital et al., 2010b) and properties (Dhital et al., 2011) of maize and potato starch have been well studied. Small granules of potato starch are digested to a higher extent than larger granules whereas the difference in rate and extent of amylolysis between granule size fractions of maize starch is not significant. In maize starch, the apparent available surface area (as represented by granule size) is relatively unimportant due to the presence of surface pores and channels, whereas the available surface area plays a major role in potato starch granules lacking pores and interior channels. Similar to maize starch and consistent with a functional role for surface pores, the differences in rate and extent of digestion between the sedimentation fractions of rice starch granules are mostly not significant. The biggest difference is observed for IR36, where larger granules have a 1.6 times lower digestion rate coefficient than small granules (Table 3). Comparatively few but larger pores in granules together with the absence of fused granule agglomerates might have resulted in the higher digestibility of smaller granules of IR36 (Fig. 4). Likewise, the agglomeration of granules does not necessarily restrict the available surface area or provide a barrier towards amylase action as these granules were observed with varying degree of cracks, fissures and irregular undulations (also observed by Wei et al. (2010) in high amylose rice starch) on the surface of granules (Figs. 7B and 9B) which may lead to an increase in effective surface area. This however differs from the results of Man et al. (2012, 2013) who described a lower amylase susceptibility of fused granule agglomerates from high amylose rice starch compared with the wild type cultivar as a function of granule size. However, comparing enzyme susceptibly between different varieties (wild-type vs. high amylose) in terms of granule size may negate the contribution made by other structural features. For example, the difference in extent of digestibility of larger (mostly fused agglomerates) and smaller (mostly individual) granules in IR36ae (Fig. 7A and B) and ami-BEIIb (Fig. 9A and B) is minimal compared to that of IR36 (Fig. 6A and B) without agglomerates (Fig. 4). Agglomerates are composed of a bundle of individual granules fused together (Shannon & Garwood, 1984) (Fig. 2F). The action of amylase on these agglomerates apparently involves initial hydrolysis and fragmentation of the outer boundary layers (Figs. 7–9B1) detaching the individual granules, allowing further hydrolysis of exposed granules by an inside-out digestion pattern similar to that of individual granules.

4.5. Thermal properties and crystalline pattern

The effect of granule size on heat stability as reflected by ΔT and amount of ordered structure as reflected by ΔH is not marked and statistically insignificant in most cases. Nevertheless, the increase of ΔH in parallel with decrease in ΔT in small granules of B- and C-polymorphic starches (Table 2) suggests more uniform crystallites in these granules compared to larger granules possibly associated

with the presence of agglomerates. As with thermal properties, the X-ray diffraction patterns (Fig. 3) for individual size fractions of the same starch are also very similar, which is different to our previous findings for maize and potato starches (Dhital et al., 2011) where larger granules had more crystalline and double helical structure. In potato starch, the peak intensity at 5.4 2θ increased markedly with granule size, however, no such specific change in peak intensity is observed in the case of B-polymorphic rice starches suggesting that the crystallinity in rice starches is not developed (annealed) slowly during the course of granule deposition as proposed for potato starch (Dhital et al., 2011). The gelatinisation temperature of starch has been positively correlated to the branch-chain length of amylopectin, longer chain lengths displaying higher gelatinisation temperature (Shi & Seib, 1995; Yuan, Thompson, & Boyer, 1993) with some exceptions such as potato starch which is thought to be affected by negatively charged phosphate monoester derivatives. Overall, the similar thermal behaviour and diffraction pattern for large and small fractions of each rice starch suggests that the effect of cellular developmental gradient and physiological age in rice starch is much less than in maize or potato starches.

5. Conclusion

The interrelation between factors responsible for enzymatic hydrolysis of rice starch granules have been demonstrated using granules isolated from both *Japonica* and *Indica* wild-types and related mutants and transgenic lines, and after sedimentation fractionation. Mutant and transgenic lines with B- and C-type crystalline polymorphs have a greater proportion of fused granule agglomerates compared to wild types with A-type crystallinity. In spite of different crystalline types, surface pores and interior channels are observed in granules from all lines, particularly after partial amylolysis. However, B-type granules are more resistant to enzymatic digestion compared to A-type granules, showing that crystalline polymorph can influence amylolysis rate independent of the presence of surface pores. It is likely that starch granule crystallinity and digestibility differences between the rice starches studied are due to small but significant differences in amylopectin branch length for *Japonica* (Butardo et al., 2011) and *Indica* (Butardo et al., 2012) lines. Whilst the present study only considered rice starch granules, the result obtained illustrate the complex interplay between molecular structure (amylopectin branch length), crystalline polymorph, and microscopic features of granules such as surface pores and interior channels in determining amylase hydrolysis features. Such a multitude of potential control points may have biological benefit in providing plants with a number of routes to tailoring the rate of starch granule hydrolysis during the germination process to respond to different environments. We can also use the information generated in this study to develop rice grains with altered digestibility and tailored functional properties.

Acknowledgements

The authors thank Dr Matthew Morell for valuable comments and suggestions, and acknowledge the facilities and the scientific and technical assistance of Dr. Kim Sewell, of the Australian Microscopy & Microanalysis Research Facility at the Centre for Microscopy and Microanalysis, The University of Queensland. This work was funded by CSIRO, The University of Queensland, and the Australian Research Council Centre of Excellence in Plant Cell Walls.

References

Al-Rabadi, G. J. S., Gilbert, R. G., & Gidley, M. J. (2009). Effect of particle size on kinetics of starch digestion in milled barley and sorghum grains by porcine alpha-amylase. *Journal of Cereal Science*, *50*(2), 198–204.

Benmoussa, M., Hamaker, B. R., Huang, C. P., Sherman, D. M., Weil, C. F., & BeMiller, J. N. (2010). Elucidation of maize endosperm starch granule channel proteins and evidence for plastoskeletal structures in maize endosperm amyloplasts. *Journal of Cereal Science*, *52*(1), 22–29.

Bird, A. R., Lopez-Rubio, A., Shrestha, A. K., & Gidley, M. J. (2009). Resistant starch in vitro and in vivo: Factors determining yield, structure and physiological relevance. In S. Kasapis, I. T. Norton, & J. B. Ubbink (Eds.), *Modern biopolymer science* (pp. 449–510). UK: Elsevier.

Butardo, V. M., Jr., Daygon, V. D., Colgrave, M. L., Campbell, P. M., Resurreccion, A., Cuevas, R. P., et al. (2012). Biomolecular analyses of starch and starch granule proteins in the high-amylose rice mutant *Goami 2*. *Journal of Agricultural and Food Chemistry*, *60*(46), 11576–11585.

Butardo, V. M., Fitzgerald, M. A., Bird, A. R., Gidley, M. J., Flanagan, B. M., Larroque, O., et al. (2011). Impact of down-regulation of starch branching enzyme IIb in rice by artificial microRNA- and hairpin RNA-mediated RNA silencing. *Journal of Experimental Botany*, *62*(14), 4927–4941.

Cai, L., & Shi, Y.-C. (2013). Self-assembly of short linear chains to A- and B-type starch spherulites and their enzymatic digestibility. *Journal of Agricultural and Food Chemistry*, *61*(45), 10787–10797.

Cai, L., & Shi, Y.-C. (2014). Preparation, structure, and digestibility of crystalline a- and b-type aggregates from debranched waxy starches. *Carbohydrate Polymers*, *105*, 341–350.

Cardoso, M. B., Putaux, J. L., Samios, D., & da Silveira, N. P. (2007). Influence of alkali concentration on the deproteinization and/or gelatinization of rice starch. *Carbohydrate Polymers*, *70*(2), 160–165.

Colonna, P., Leloup, V., & Buleon, A. (1992). Limiting factors of starch hydrolysis. *European Journal of Clinical Nutrition*, *46*, S17–S32.

Dhital, S., Shelat, K. J., Shrestha, A. K., & Gidley, M. J. (2013). Heterogeneity in maize starch granule internal architecture deduced from diffusion of fluorescent dextran probes. *Carbohydrate Polymers*, *93*(2), 365–373.

Dhital, S., Shrestha, A. K., & Gidley, M. J. (2010a). Effect of cryo-milling on starches: Functionality and digestibility. *Food Hydrocolloids*, *24*(2–3), 152–163.

Dhital, S., Shrestha, A. K., & Gidley, M. J. (2010b). Relationship between granule size and in vitro digestibility of maize and potato starches. *Carbohydrate Polymers*, *82*(2), 480–488.

Dhital, S., Shrestha, A. K., Hasjim, J., & Gidley, M. J. (2011). Physicochemical and structural properties of maize and potato starches as a function of granule size. *Journal of Agricultural and Food Chemistry*, *59*(18), 10151–10161.

Evans, A., & Thompson, D. B. (2004). Resistance to alpha-amylase digestion in four native high-amylose maize starches. *Cereal Chemistry*, *81*(1), 31–37.

Fannon, J. E., Hauber, R. J., & BeMiller, J. N. (1992). Surface pores of starch granules. *Cereal Chemistry*, *69*(3), 284–288.

Fannon, J. E., Shull, J. M., & BeMiller, J. N. (1993). Interior channels of starch granules. *Cereal Chemistry*, *70*(5), 611–613.

Franco, C. M. L., & Ciacco, C. F. (1992). Factors that affect the enzymatic degradation of natural starch granules – effect of the size of the granules. *Starch-Starke*, *44*(11), 422–426.

Franco, C. M. L., Ciacco, C. F., & Tavares, D. Q. (1998). The structure of waxy corn starch: Effect of granule size. *Starch-Starke*, *50*(5), 193–198.

Fukai, Y., Takaki, E., & Kobayashi, S. (1994). Changes in 3 kinds of starch granules after enzymatic treatment. *Nippon Nogeikagaku Kaishi-Journal of the Japan Society for Bioscience Biotechnology and Agrochemistry*, *68*(4), 793–800.

Gallant, D. J., Bouchet, B., & Baldwin, P. M. (1997). Microscopy of starch: Evidence of a new level of granule organization. *Carbohydrate Polymers*, *32*(3–4), 177–191.

Gallant, D. J., Bouchet, B., Buleon, A., & Perez, S. (1992). Physical characteristics of starch granules and susceptibility to enzymatic degradation. *European Journal of Clinical Nutrition*, *46*, S3–S16.

Gerard, C., Colonna, P., Buleon, A., & Planchot, V. (2001). Amylolysis of maize mutant starches. *Journal of the Science of Food and Agriculture*, *81*(13), 1281–1287.

Gott, B., Barton, H., Samuel, D., & Torrence, R. (2006). Biology of starch. In R. Torrence, & H. Barton (Eds.), *Ancient starch research* (pp. 35–45). Walnut Creek, CA, USA: Left Coast Press.

Hu, P., Zhao, H., Duan, Z., Linlin, Z., & Wu, D. (2004). Starch digestibility and the estimated glycemic score of different types of rice differing in amylose contents. *Journal of Cereal Science*, *40*(3), 231–237.

Huber, K. C., & BeMiller, J. N. (2000). Channels of maize and sorghum starch granules. *Carbohydrate Polymers*, *41*(3), 269–276.

Jane, J. L., Wong, K. S., & McPherson, A. E. (1997). Branch-structure difference in starches of A- and B-type X-ray patterns revealed by their Naegeli dextrins. *Carbohydrate Research*, *300*(3), 219–227.

Man, J., Yang, Y., Huang, J., Zhang, C., Zhang, F., Wang, Y., et al. (2012). Morphology and structural properties of high-amylose rice starch residues hydrolyzed by amyloglucosidase? *Food Chemistry*, *138*(4), 2089–2098.

Man, J., Yang, Y., Huang, J., Zhang, C., Zhang, F., Wang, Y., et al. (2013). Morphology and structural properties of high-amylose rice starch residues hydrolyzed by porcine pancreatic alpha amylase. *Food Hydrocolloids*, *13*, 195–203.

Morita, T., Ito, Y., Brown, I. L., Ando, R., & Kiriyama, S. (2007). *In vitro* and *in vivo* digestibility of native maize starch granules varying in amylose contents. *Journal of AOAC International*, *90*(6), 1628–1634.

Nakamura, Y., Francisco, P. B., Hosaka, Y., Sato, A., Sawada, T., Kubo, A., et al. (2005). Essential amino acids of *Starch Synthase IIa* differentiate amylopectin structure and starch quality between Japonica and Indica rice varieties. *Plant Molecular Biology*, *58*(2), 213–227.

Noda, T., Takigawa, S., Matsuura-Endo, C., Kim, S. J., Hashimoto, N., Yamauchi, H., et al. (2005). Physicochemical properties and amylopectin structures of large,

small, and extremely small potato starch granules. *Carbohydrate Polymers*, *60*(2), 245–251.
Payan, F., Haser, R., Pierrot, M., Frey, M., Astier, J. P., Abadie, B., et al. (1980). 3-Dimensional structure of alpha-amylase from porcine pancreas at 5-A resolution-active-site location. *Acta Crystallographica*, *36*, 416–421.
Planchot, V., Colonna, P., & Buleon, A. (1997). Enzymatic hydrolysis of alpha-glucan crystallites. *Carbohydrate Research*, *298*(4), 319–326.
Ring, S. G., Gee, J. M., Whittam, M., Orford, P., & Johnson, I. T. (1988). Resistant starch – its chemical form in foodstuffs and effect on digestibility *in vitro*. *Food Chemistry*, *28*(2), 97–109.
Shannon, J. C., & Garwood, D. L. (1984). Genetics and physiology of starch development. In R. L. Whistler, J. N. Bemiller, & E. F. Paschall (Eds.), *Starch chemistry and technology* (pp. 25–86). New York: Academic Press.
Shapter, F. M., Henry, R. J., & Lee, L. S. (2008). Endosperm and starch granule morphology in wild cereal relatives. *Plant Genetic Resources Characterization and Utilization*, *6*(2), 85–97.
Shi, Y. C., & Seib, P. A. (1995). Fine-structure of maize starches from 4 wx-containing genotypes of the W64A inbred line in relation to gelatinization and retrogradation. *Carbohydrate Polymers*, *26*(2), 141–147.
Shrestha, A. K., Blazek, J., Flanagan, B. M., Dhital, S., Larroque, O., Morell, M. K., et al. (2012). Molecular, mesoscopic and microscopic structure evolution during amylase digestion of maize starch granules. *Carbohydrate Polymers*, *90*(1), 23–33.
Tang, H., Ando, H., Watanabe, K., Takeda, Y., & Mitsunaga, T. (2001). Fine structures of amylose and amylopectin from large, medium, and small waxy barley starch granules. *Cereal Chemistry*, *78*(2), 111–115.
Umemoto, T., Aoki, N., Lin, H., Nakamura, Y., Inouchi, N., Sato, Y., et al. (2004). Natural variation in rice *Starch Synthase IIa* affects enzyme and starch properties. *Functional Plant Biology*, *31*(7), 671–684.
Warren, F. J., Royall, P. G., Gaisford, S., Butterworth, P. J., & Ellis, P. R. (2011). Binding interactions of α-amylase with starch granules: The influence of supramolecular structure and surface area. *Carbohydrate Polymers*, *86*(2), 1038–1047.
Wei, C., Qin, F., Zhu, L., Zhou, W., Chen, Y., Wang, Y., et al. (2010). Microstructure and ultrastructure of high-amylose rice resistant starch granules modified by antisense RNA inhibition of starch branching enzyme. *Journal of Agricultural and Food Chemistry*, *58*(2), 1224–1232.
Yuan, R. C., Thompson, D. B., & Boyer, C. D. (1993). Fine-structure of amylopectin in relation to gelatinization and retrogradation behavior of maize starches from 3 wx-containing genotypes in 2 inbred lines. *Cereal Chemistry*, *70*(1), 81–89.
Zhang, B., Dhital, S., & Gidley, M. J. (2013). Synergistic and antagonistic effects of α-amylase and amyloglucosidase on starch digestion. *Biomacromolecules*, *14*(6), 1945–1954.
Zhang, G. Y., Ao, Z. H., & Hamaker, B. R. (2006). Slow digestion property of native cereal starches. *Biomacromolecules*, *7*(11), 3252–3258.
Zhang, G., Venkatachalam, M., & Hamaker, B. R. (2006). Structural basis for the slow digestion property of native cereal starches. *Biomacromolecules*, *7*(11), 3259–3266.
Zhu, L.-J., Liu, Q.-Q., Wilson, J. D., Gu, M.-H., & Shi, Y.-C. (2011). Digestibility and physicochemical properties of rice (*Oryza sativa* L.) flours and starches differing in amylose content. *Carbohydrate Polymers*, *86*(4), 1751–1759.